Optimising view angles for the estimation of leaf area index via entropy-difference analysis

Yanjuan Yao[1,2,*], Qiang Liu[1,3], Qinhuo Liu[1] and Yanhua Gao[1,2]

[1]*Institute of Remote Sensing Applications (IRSA), Chinese Academy of Sciences (CAS), Beijing, China.*
[2]*Satellite Environment Center (SEC), Ministry of Environmental Protection (MEP) of China, Beijing, China.*
[3]*College of Global Change and Earth System, Beijing Normal University, Beijing, China.*
[*]*Corresponding author. e-mail: yjyao2008@yahoo.com.cn*

It is important to evaluate the information content of remote sensing data in order to synthetically use multi-source remote sensing data to improve the accuracy and consistency of land surface parameter retrieval. This paper presents a technique for information content evaluation of multi-spectral/angular remote sensing data for the leaf area index (LAI) inversion, the method of entropy-difference analysis. The proposed method is based on a numerical evaluation of the entropy of the observed dataset to learn how much variation in observation is caused by the variation in LAI. The relationship between remote sensing information and the LAI inversion accuracy is validated based on the model-simulated canopy reflectance data and the experiment data. We make the following observation: the larger the entropy-difference for canopy reflectance data, the higher the LAI inversion accuracy. That is, choosing a good combination of observation angles is sometimes more important than simply increasing the number of observations. The presented technique may be useful in designing and evaluating quantitative remote sensing algorithms and products.

1. Introduction

The leaf area index (LAI) is one of the key ecological parameters used not only for global-scale, but also for local-scale vegetation monitoring (Yang *et al* 2007; Gao *et al* 2008). Remote sensing has been demonstrated to have wide applicability in mapping the LAI over large areas. Recent advances have shown that it is possible to combine multiple source reflectance data to improve product accuracy and reduce the missing data frequency (Deng *et al* 2006). Currently, vegetation canopy reflectance is measured by a variety of sensors mounted on aircrafts and satellites (Canisius *et al* 2010). Both directional and spectra information are very important for inferring canopy properties based on radiative transfer models (Bicheron and Leroy 1999).

In fact, the available remote sensing data are usually correlated when the bandpass and view angles are similar. To reduce data redundancies, it is important to select the optimal wavelength and view angle while maintaining the desirable LAI inversion accuracy. The optimal selection for multi-band/angle remote sensing data could be done using sensitivity analysis methods (Goel and Strebel 1983; Privette *et al* 1996; Yao *et al* 2008), iterative inversion techniques (Gao and Lesht 1997; Weiss *et al* 2000; Lozano *et al* 2009), or information content-based methods (Jin *et al* 2002).

Keywords. Information evaluation; multi-angular/spectral remote sensing; entropy-difference analysis; leaf area index inversion.

The sensitivity analysis indicates which band or direction is most sensitive to a particular parameter of the model. However, when we use a combination of multiple remote sensing observations to invert more than one parameter, the correlations within the data samples and the entangling effects among the parameters must be considered. As a result, this complicated problem may be disentangled by sensitivity analysis alone, but this strategy is not straightforward according to current knowledge. Although it is possible to study optimal data selection by iterative inversion techniques (Gao and Lesht 1997; Weiss *et al* 2000; Lozano *et al* 2009), the result will be specific to the particular dataset, and an enormous amount of calculation is needed. Jin *et al* (2002) investigated the inversion results for different remote sensing data based on a linear kernel-driven model to explore the information content. However, the information content for the nonlinear physical model is limited.

The LAI inversions based on multi-source remote sensing data require an information content evaluation to determine the data optimal selection and to reduce data redundancy without losing the parameter inversion accuracy. Here, we propose a technique called the entropy-difference analysis, which is based on the information theory, to evaluate the information content of remote sensing data for the LAI inversion.

2. The entropy-difference analysis method

2.1 *Entropy-difference definition for canopy reflectance data*

Entropy is often taken as the amount of related information for a random variable in the information theory. Shannon's information entropy (Woodbury and Ulrych 1993) is applied to calculate entropy here. Generally, the observed canopy reflectance data in a spectral band at n fixed sun-view configuration are assumed to be one of the random signals that obey the n-dimensional Gaussian distribution. The entropy of canopy reflectance data can be calculated as follows:

$$H\left(r_{\mathrm{CR}}\right)=\frac{1}{2}\log\left|M\right|+\frac{n}{2}\log\left(2\pi e\right) \tag{1}$$

where r_{CR} denotes the random signal of directional canopy reflectance, r_{CR}=($r_{\mathrm{CR}_1}, r_{\mathrm{CR}_2}, \ldots, r_{\mathrm{CR}_n}$), and n is the number of sun-view samples in canopy reflectance data. We say that r_{CR} is a random sample in the set of all possible values of canopy reflectance data, $r_{\mathrm{CR}} \in \Omega$, where Ω denotes the set of all possible values. In this view, the statistics of r_{CR} can be derived. M is the covariance matrix of r_{CR}, and $|M|$ denotes the determinant of the covariance matrix M. π and e are constants.

The entropy-difference (ΔH) with respect to the LAI inversion in remote sensing is computed based on the following formula:

$$\Delta H=H_2-H_1=\frac{1}{2}\log\frac{\left|M_2\right|}{\left|M_1\right|} \tag{2}$$

where H_2 refers to the entropy when $r_{\mathrm{CR}}\in\Omega_2$. Ω_2 denotes the set of all possible values of canopy reflectance data in the natural state. H_1 refers to the entropy when $r_{\mathrm{CR}} \in \Omega_1$. Ω_1 is a subset of Ω_2 in which the LAI is fixed to the value of *a priori* mean, i.e., $\Omega_1 = \{r_{\mathrm{CR}} | r_{\mathrm{CR}} \in \Omega_2 \text{ and } \mathrm{LAI} = \mathrm{LAI}_0\}$. $|M_2|$ and $|M_1|$ are the determinants corresponding to H_2 and H_1, respectively. The larger the entropy-difference is, the more information for the LAI is contained in the canopy reflectance data.

2.2 *Understanding entropy-difference in view of the BRDF model*

The BRDF model for canopy reflectance can be written as:

$$R_i=R\left(\mathrm{X},\mathrm{P},\theta_v\left(i\right),\theta_s\left(i\right),\varphi\left(i\right)\right) \tag{3}$$

where R_i denotes the directional canopy reflectance. i indicates the solar/view directions, and i=1, 2, …, n. X is a vector of unknown parameters that we are trying to retrieve by inverting the BRDF model based on a set of observed canopy reflectances. P is a vector of parameters that can be fixed (either known or insensitive in the model). $\theta_v(i)$, $\theta_s(i)$ and $\varphi(i)$ are the view zenith, solar zenith and relative azimuth angles for observation i, respectively.

For the sake of simplifying our analysis, we introduce a linear approximation to the canopy reflectance model. That is, $\Delta\,(\Delta=\mathrm{X}-\mathrm{X}_0)$ is small enough so that near the *a priori* mean vector X_0, using linear approximation, the BRDF model can be rewritten as:

$$\begin{aligned}R_i=&R'\left(\mathrm{X}_0,\mathrm{P},\theta_v\left(i\right),\theta_s\left(i\right),\varphi\left(i\right)\right)\left(\mathrm{X}-\mathrm{X}_0\right)\\&+R\left(\mathrm{X}_0,\mathrm{P},\theta_v\left(i\right),\theta_s\left(i\right),\varphi\left(i\right)\right)\end{aligned} \tag{4}$$

where R' is the BRDF model partial derivatives for X_0.

A sample of the observed value of canopy reflectance can be written as:

$$\hat{R} = R'\left(\mathrm{X}_0, \mathrm{P}, \theta_v\left(i\right), \theta_s\left(i\right), \varphi\left(i\right)\left(\mathrm{X} - \mathrm{X}_0\right)\right) + R\left(\mathrm{X}_0, \mathrm{P}, \theta_v\left(i\right), \theta_s\left(i\right), \varphi\left(i\right)\right) + \xi \quad (5)$$

where ξ refers to the noise in the observed data, which we assume is Gaussian noise with a zero mean and standard deviation σ_ξ. To simplify the formula, we define

$$\begin{aligned} B_i &= \hat{R} - R\left(\mathrm{X}_0, \mathrm{P}, \theta_v\left(i\right), \theta_s\left(i\right), \varphi\left(i\right)\right), \\ A_i &= R'\left(\mathrm{X}_0, \mathrm{P}, \theta_v\left(i\right), \theta_s\left(i\right), \varphi\left(i\right)\right), \\ i &= 1, 2, \ldots, n \end{aligned} \quad (6)$$

when B is the observation vector, B is the vector of B_i, A means the sensitivity matrix, and A is the vector of A_i. Equation (5) can then be rewritten as:

$$B = A\mathrm{Y} + \xi \quad (7)$$

Here, we call Y the vector of unknown parameters, and $\mathrm{Y} = \mathrm{X} - \mathrm{X}_0$.

For the sake of simplification and without loss of generality, we consider the BRDF model to have only two unknown parameters. The first one is our target parameter (LAI), and the second one is a disturbance parameter to the inversion process. The other parameters are assumed to be constants. When there are two unknown parameters in the vector Y, equation (7) can be written as:

$$B = \left(A_1\ A_2\right)\begin{pmatrix} Y_1 \\ Y_2 \end{pmatrix} + \xi. \quad (8)$$

When the target parameter (LAI) is fixed to its *a priori* mean value (LAI_0), Y_1 is zero and equation (8) becomes:

$$B = \left(A_1\ A_2\right)\begin{pmatrix} 0 \\ Y_2 \end{pmatrix} + \xi. \quad (9)$$

Equations (8) and (9) are the starting equations to derive the entropy-difference formula.

The covariance matrix for the canopy reflectance data (r_{CR}) can be explicitly calculated as follows:

$$M = \mathrm{Cov}\left(B\right) = \sigma_1^2 A_1 A_1^T + \sigma_2^2 A_2 A_2^T + \sigma_\xi^2 I \quad (10)$$

where σ_1, σ_2 and σ_ξ are the standard deviations of the unknown parameters Y_1, Y_2 and ξ, respectively. I is an identity matrix.

When entropy-difference is computed, two cases will be considered here; i.e., for the angle constitution of the remote sensing data, there are two or three angles in the canopy reflectance data. We take only these cases as an example because the formula for data of more angles is similar to that used for this case.

Based on equations (2), (8), (9) and (10), when there are two angles in the canopy reflectance data, the entropy-difference is calculated by:

$$\Delta H = \frac{1}{2}\log\left(\frac{\left[\left(A_{1,2}A_{2,1} - A_{1,1}A_{2,2}\right)^2\sigma_1^2\sigma_2^2 + \left(A_{2,2}^2 + A_{2,1}^2\right)^2\sigma_\xi^2\sigma_2^2 + \left(A_{1,1}^2 + A_{1,2}^2\right)\sigma_\xi^2\sigma_1^2 + \sigma_\xi^2\sigma_\xi^2\right]}{\left[\left(A_{2,1}^2 + A_{2,2}^2\right)\sigma_2^2 + \sigma_\xi^2\right]\sigma_\xi^2}\right). \quad (11)$$

When there are three angles in the canopy reflectance data, the entropy-difference is calculated by:

$$\Delta H = \frac{1}{2}\log\left(\frac{\left\{\left[\left(A_{1,3}A_{2,2} - A_{1,2}A_{2,3}\right)^2 + \left(A_{2,1}A_{1,3} - A_{1,1}A_{2,3}\right)^2 + \left(A_{2,1}A_{1,2} - A_{1,1}A_{2,2}\right)^2\right]\sigma_1^2\sigma_2^2 + \left(A_{1,1}^2 + A_{1,2}^2 + A_{1,3}^2\right)\sigma_\xi^2\sigma_1^2 + \left(A_{2,1}^2 + A_{2,2}^2 + A_{2,3}^2\right)\sigma_\xi^2\sigma_2^2 + \sigma_\xi^2\sigma_\xi^2\right\}}{\left[\left(A_{2,1}^2 + A_{2,2}^2 + A_{2,3}^2\right)\sigma_2^2 + \sigma_\xi^2\right]\sigma_\xi^2}\right) \quad (12)$$

where σ_1, σ_2, and σ_ξ are the standard deviations of the target parameter, the disturbance parameter, and the noise in the observation, respectively. $A_{i,j}$ indicates the parameter sensitivity of the canopy reflectance model, i indicates the parameter, and j indicates the observation angle. $A_{1,2}A_{2,1} - A_{1,1}A_{2,2}$ and $\left(A_{1,3}A_{2,2} - A_{1,2}A_{2,3}\right)^2 + \left(A_{2,1}A_{1,3} - A_{1,1}A_{2,3}\right)^2 + \left(A_{2,1}A_{1,2} - A_{1,1}A_{2,2}\right)^2$ correspond to the correlation sensitivity for the two/three unknown parameters. $A_{1,1}^2 + A_{1,2}^2$ and $A_{1,1}^2 + A_{1,2}^2 + A_{1,3}^2$ correspond to the sensitivity of the target parameter (LAI). $A_{2,2}^2 + A_{2,1}^2$ and $A_{2,1}^2 + A_{2,2}^2 + A_{2,3}^2$ correspond to the sensitivity of the disturbance parameter.

From equations (11) and (12), the factors affecting the entropy difference for the canopy reflectance data can be expressed explicitly as follows:

The first and important factor is the data quality (σ_ξ), which is represented by the SNR (signal-to-noise ratio) of the sensor. The second factor is the uncertainty range of model parameters, which varies because of the diversity of the surface. Third, the sensitivities of parameters in the BRDF model, which indicate the parameters' role in the model are important. Last, the correlation between the sensitivity of the parameters affects the information content in the canopy reflectance data.

3. Application of the LAI inversion

Entropy-difference is a quantitative measurement of the information content in canopy reflectance data with respect to parameter inversion. One key question is whether canopy reflectance data with more information content will result in the higher accuracy of the LAI estimation. In this section, we will investigate this argument.

3.1 *Model and inversion method*

The canopy BRDF model used here is a typical radiative transfer model, SAIL (Verhoef 1984). The SAIL model was chosen because it has not only been widely tested but also offers a good representation of a homogeneous canopy with a limited number of input parameters and a reasonable computation time (Goel and Deering 1989; Major *et al* 1992).

The input parameters in the SAIL model are the following:

- spectral parameters: leaf reflectance (ρ_l) and transmittance (τ_l), soil reflectance (ρ_s), and ratio of diffuse to direct irradiation (SKYL)
- structural parameters: leaf area index (LAI) and leaf inclination angle distribution (LAD)
- solar/view geometry: solar zenith angle (SZA), solar azimuth angle (SAA), view zenith angle (VZA), and view azimuth angle (VAA).

Model inversion in remote sensing usually causes ill-posed problems. The Bayes theory is a good way to incorporate *a priori* knowledge into model inversion (Yao *et al* 2008; Li *et al* 2001). The Bayesian inversion method is used in this paper. The parameters with large uncertainty range and large sensitivity should be inverted (Goel and Strebel 1983). Based on analysis with field measured canopy reflectance data, we chose the LAI and soil reflectance ρ_s as the two parameters that need to be inverted. We assume that in addition to random noise, the uncertainty of the LAI and ρ_s cause the variation in the observed canopy reflectance data.

In this study, we considered three typical crop growth stages: the early growth stage, the advanced growth stage, and the fully developed canopy stage. In the early growth stage, which includes the seedling stage, the trileaf stage, and the ten leaf stage, the *a priori* mean of LAI is 0.5 and the ground is partially covered by leaf. In the advanced growth stage, including the elongation stage, the *a priori* mean of LAI is 2 and the ground is almost covered by leaf. In the fully developed canopy stage, which comprises the late elongation stage, the pregnation stage, and the tasseling stage, the *a priori* mean of LAI is 4, the ground is all covered by leaf, and the canopy reflectance is saturated with respect to LAI inversion according to the literature (Bicheron and Leroy 1999; Weiss *et al* 2000).

For a typical crop land, LAI is distributed in some uncertain range according to the growth stage of the crop. Soil reflectance has a range of variation too because of the soil type diversity, texture, and the soil moisture difference. Considering the diversity of the natural surface, we investigated two typical settings of uncertainty (distinguished by their standard deviations) for LAI (stds. are 0.293 and 0.1465) and the soil reflectance (stds. are 0.01466 and 0.005857). As to the noises in canopy reflectance data, we assumed that they have a Gaussian distribution. The combinations of these cases result in eight cases of uncertainty settings (see table 1). In table 1, ε represents the relative noise level with respect to the average canopy reflectance. It means that the standard deviation of noise in a spectral band is the product of ε and the average canopy reflectance in this spectral band if there is no noise.

Other parameters of the model are the same as those in Yao *et al* (2008). That is, the solar zenith and azimuth angles are 22.12° and 135.32°, respectively. Spectral properties of corn leaf and soil were measured with the Analytical Spectral Devices (ASD 2000) which covers the spectrum range of 0.35–2.5 μm. The most commonly used bands for vegetation monitoring are red and near-infrared (NIR) bands. The reflectance and transmittance of the leaf (ρ_l and τ_l) are 0.079 and 0.036 in red band, and 0.431 and 0.530 in NIR band. The mean reflectance of soil is 0.163 in red band and 0.209 in NIR band, but its actual value is randomly distributed according to table 1. The SKYL is set to 0.12 in both red and NIR bands. LAI values are also randomly generated according to the three growth stages (early growth stage; advanced growth stage; fully developed canopy) and the standard deviation in table 1. Leaf angel distribution (LAD) is

Table 1. *Eight cases for uncertainty of parameters for entropy-difference calculation.*

Case no.	Std. of LAI	Std. of ρ_{soil}	ε (%)
I	0.293	0.01466	0.005
II	0.293	0.005857	0.005
III	0.1465	0.01466	0.005
IV	0.1465	0.005857	0.005
V	0.293	0.01466	1
VI	0.293	0.005857	1
VII	0.1465	0.01466	1
VIII	0.1465	0.005857	1

fixed to its measured value for corn leaf in Huailai RS Experiment Station, and is expressed by the ellipsoidal distribution function (Campbell 1985).

3.2 *Information content distribution*

To examine the distribution of information content with respect to view angle, the entropy differences of canopy reflectance data for NIR bands in the principal plane (the std. of LAI, ρ_{soil} and ε (%) is 0.293, 0.01466 and 0.005, respectively) are presented in figure 1, illustrating the information distribution for the first angle, the second angle (based on the first optimal angle), and the third angle (based on the first and second optimal angles).

For information content distribution of one view angle, when the *a priori* mean LAI is low (0.5, early growth stage), the entropy-difference generally increases with a larger view zenith angle, so the optimal angle occurs at the large view zenith angle. When the *a priori* mean LAI is high (2 and 4, advanced and fully developed growth stages), the trend is different. With increasing view zenith angle, the entropy difference increases, reaching the maximum value at a certain view zenith angle and then decreases. The optimal angle does not occur at the largest view zenith angle, which means that

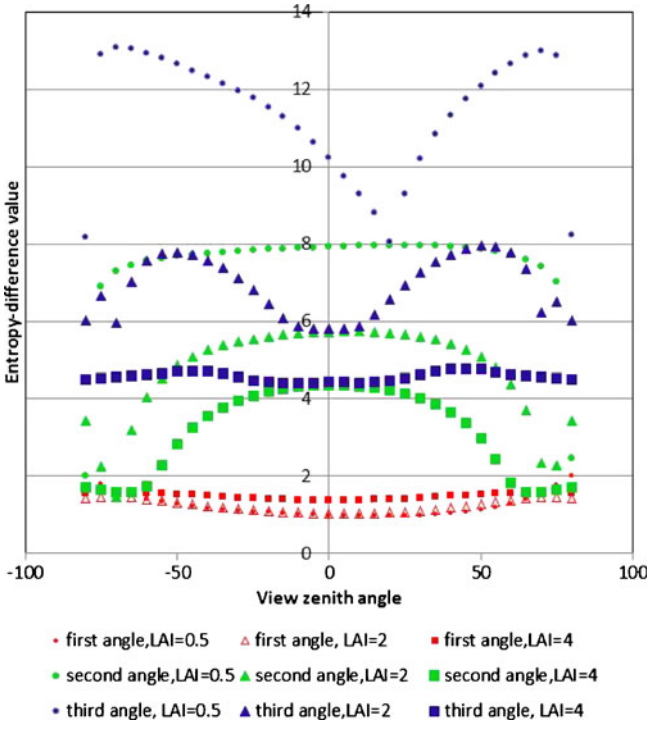

Figure 1. The information content distribution for the NIR band in the principal plane for different crop growth stages. Note: Solar azimuth angle and zenith angle are 135.32 and 22.12, respectively. A negative view zenith angle indicates a backward viewing direction and a positive view zenith angle indicates a forward viewing direction.

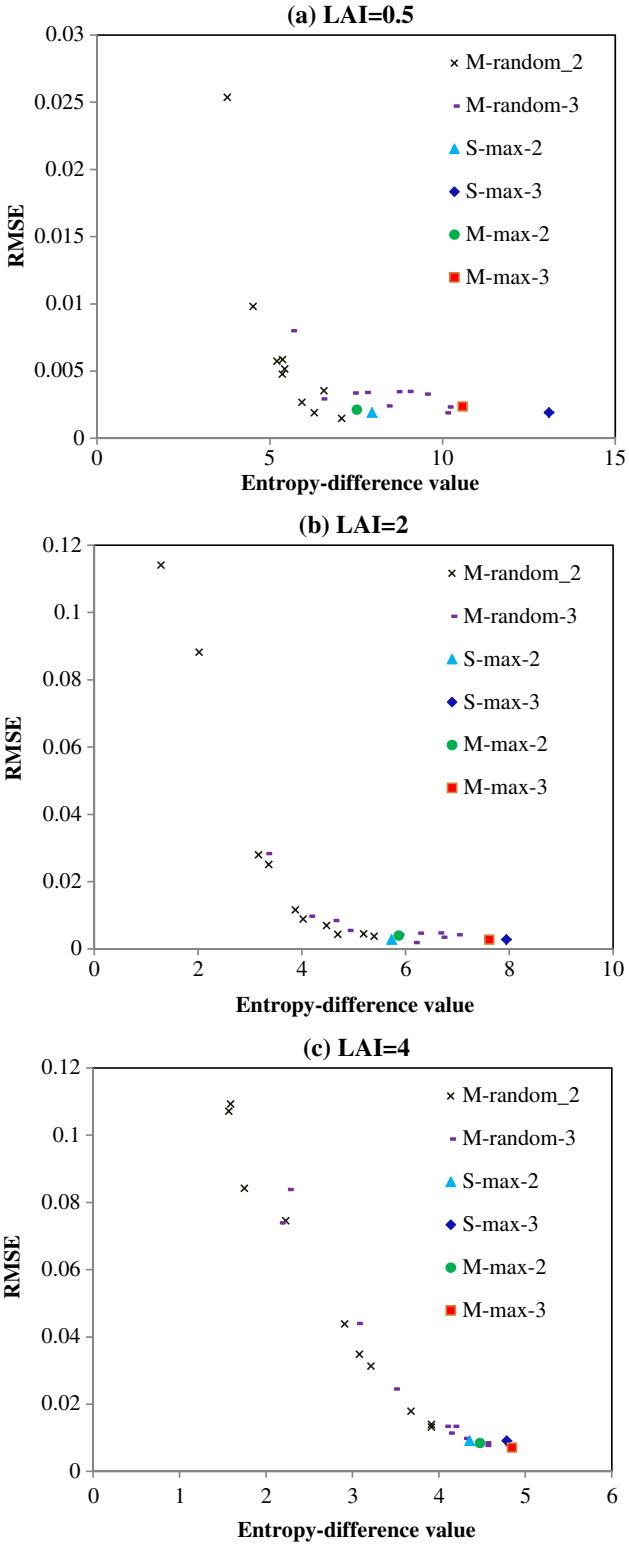

Figure 2. Scatter-plot between the entropy-difference value (information content) and RMSE for different crop growth stages (mean LAI is 0.5, 2 and 4). Note: The optimised configurations in the whole view hemisphere are denoted as 'S-max-2' and 'S-max-3' for using 2 and 3 samples, respectively; the optimised configurations for the MODIS sun/view angles are denoted as 'M-max-2' and 'M-max-3' for using 2 and 3 samples, respectively; the random angle samples from the MODIS images composite are denoted as 'M-random-2' and 'M-random-3' for using 2 and 3 samples, respectively.

the larger the *a priori* mean LAI value is, the smaller the first optimal view zenith angle.

For the information content distribution of the second view angle, the entropy-difference of the second angle is quite different than that of the first angle: the entropy-difference is larger when the second angle is close to the nadir. Thus, the entropy-difference is maximised when the second angle is complementary to the first angle. It is also worthwhile to mention that the entropy-difference of the 2-angle dataset is always larger than the 1-angle dataset. Moreover, the entropy-difference is larger when the *a priori* mean LAI is low than when the *a priori* mean LAI is high.

For the information content distribution of the third view angle, the overall entropy-difference is larger than that of the 2-angle dataset. Additionally, the information contained in the reflectance data for the low *a priori* mean LAI is larger than that for the high *a priori* mean LAI. At this time, the optimal angle configuration favours a large view zenith angle. When the *a priori* mean LAI is 4, the change in the entropy-difference is small with respect to the third angle, which may be explained by the fact that the LAI is saturated to the directional canopy reflectance.

3.3 *Application based on simulated data*

To clearly reveal the relationship between the information content of canopy reflectance data and inversion accuracy, the inversions were performed using an optimised angle sample configuration and random samples. A set of observed canopy reflectance data is simulated for each view angle with the canopy BRDF model, with parameter settings according to certain *a priori* knowledge of the model parameters' distribution. Then, the entropy-difference is computed for each view angle, and its maximum value indicates the optimal view angle. When there are two or more angles in canopy reflectance data, a recursive strategy is adopted to simplify the searching process. That is, to find the optimal angle configuration for the canopy reflectance data containing two samples, we fix the first angle to the optimal angle, which has been selected for the one-sample data, and then search the viewing hemisphere for the second optimal angle, which in combination with the first angle will generate the maximum entropy difference value. For three or more angles, the optimal angle is selected in a similar way.

We consider two situations for view angle optimisation – one is to optimise the whole viewing hemisphere (the angle is set as 5° increments of the zenith angle from 0° to 80° and 20° increments of the relative azimuth angle from 0° to 360°; this is an ideal situation but not very practical), the other is to optimise within several view angles that are currently available. As for the datasets optimised within certain available angles, for example, the view angles of 16-day MODIS (Moderate-resolution Imaging Spectroradiometer) images, compositions are used for a view angle optimisation experiment.

The settings of uncertainty in figure 2 are as follows: the std. for the LAI and ρ_s is 0.293 and 0.01466, respectively; and the relative noise level with respect to the average canopy reflectance is 0.005%. For each simulation, we created hundred datasets, with different noises according to the noise distribution. The RMSE is computed based on the inverted LAI for each of the hundred datasets to indicate the inversion accuracy of the parameters. The scatter-plot between the entropy-difference value (ΔH) and the RMSE of the LAI inversion for the NIR band is illustrated in

Table 2. *The optimal angle configuration for NIR bands.*

Growth stages	Angular set	Optimal for hemisphere (VAA/VZA)	Optimal for MODIS (SAA/SZA/VAA/VZA)
LAI=0.5	1st angle	135.32/80	133.28/36.95/90.53/64.34
	2nd angle	315.32/20	162.05/29.87/285.49/15.7
	3rd angle	135.32/70	134.05/35.25/91.58/61.26
LAI=2	1st angle	135.32/70	133.28/36.95/90.53/64.34
	2nd angle	315.32/5	156.25/30.26/112.29/3.16
	3rd angle	315.32/50	140.04/32.66/95.36/48.67
LAI=4	1st angle	135.32/65	149.16/32.42/98.7/29.75
	2nd angle	135.32/0	143.94/33.18/97.2/43.23
	3rd angle	315.32/45	140.04/32.66/95.36/48.67

Note: SAA/SZA/VAA/VZA correspond to solar azimuth angle, solar zenith angle, view azimuth angle, and view zenith angle, respectively. SAA and SZA for the optimal of the hemisphere are 135.32 and 22.12, respectively.

figure 2. The optimal angle configuration in figure 2 is shown in table 2.

From figure 2, we can see that the larger the entropy-difference for canopy reflectance data, the higher the inversion accuracy for the LAI. The inversion RMSE of the LAI is inversely proportional to the entropy-difference value. Throughout our extended test, this trend exists for band configurations, data quality, and *a priori* knowledge. We also observe that in the case of both 2-angle and 3-angle samples, the optimal configurations always have higher entropy-differences than the random samples and smaller RMSE for LAI inversion. Furthermore, the optimal configurations in the whole viewing hemisphere are better than the optimal configurations in the 16 MODIS sun/view geometries.

The entropy-difference of 3-angle data is generally higher than that of 2-angle data, but this trend is far from a strict law. In many cases, the optimal configuration of two angles has a larger entropy-difference than some random datasets of three angles. This is especially true when the LAI is high. Hence, it is more necessary to choose reflectance data with a good angle combination to invert parameters than simply to increase data containing the number of angles.

3.4 *Application based on experiment data*

In order to validate the relationship between the reflectance data information content and the LAI inversion accuracy, LAI is also inverted based on the multi-angular and multi-spectral canopy reflectance data of corn for different growth stages measured in Heihe River Basin, the second largest inland river basin in the arid regions of northwestern China (Gansu province). Various corn canopy biophysical parameters and spectral data were measured for typical growth stages at the Yingke sites (E100.410444, N38.857056) from May to July 2008. Because of the weather conditions, we obtained the experiment measurement on May 30, June 22 and July 1, 2008. Parameter measurements include LAI, LAD, soil moisture, leaf hemisphere reflectance, leaf hemisphere transmittance, soil reflectance, SKYL, canopy bidirectional reflectance, etc. The measurement methods are the same as those in Yao *et al* (2008).

LAI is inverted based on different canopy reflectance datasets containing different information, namely all canopy reflectance measurements, optimal canopy reflectance data, and randomly selected canopy reflectance data. Here, there are 56 datasets for all canopy reflectance measurements. For the optimal data combination, we considered three situations, containing 1, 2 and 3 datasets, respectively. As to each randomly selected dataset, there are many combinations and LAI is inverted for every combination. For all the inverted LAIs, we computed the mean and standard deviation. The comparison of true LAI with the inverted LAI is shown in figure 3.

From figure 3, we can see that the inverted LAI for all the reflectance measurements is consistent with the field measured LAI. The LAI inversion accuracy for the optimal datasets is also very high, especially for the dataset that contains three subsets of canopy reflectance data. Considering the balance between the computation time and the inversion accuracy, the optimal data is preferred to all the measurement data. In contrast with the optimal data, the accuracy for the random datasets is lower than that for the optimal datasets. So the

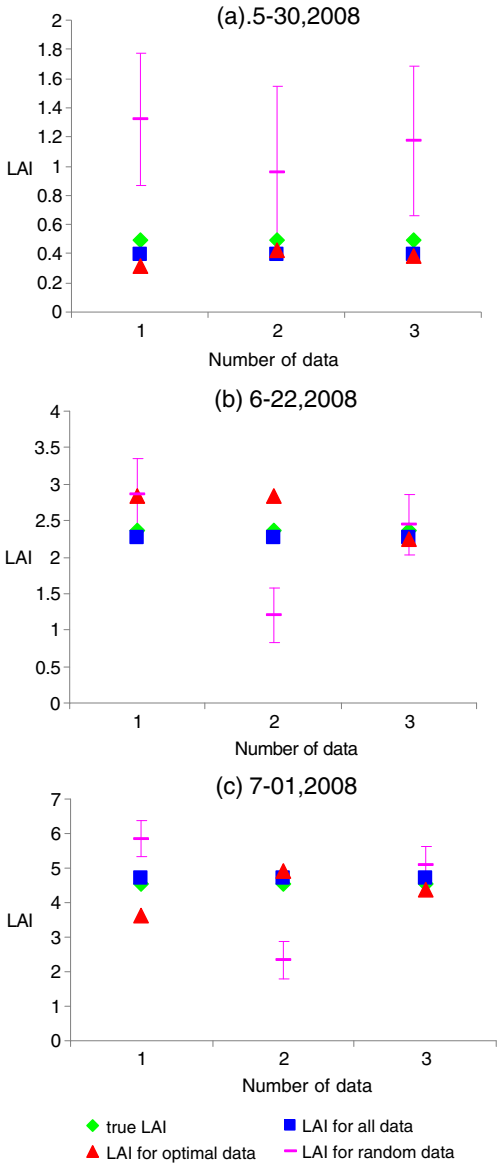

Figure 3. The comparison of field measured LAI with the inverted LAI for different data combination from field canopy reflectance measurement.

LAI inversion based on the optimal data is promising for the experiment measurement of canopy reflectance data.

4. Discussion

There are several assumptions made in this paper. To derive the formula in section 2.2, we assume that the BRDF model could be approximated locally by a linear model and that *a priori* knowledge for the target or non-target parameters is sufficient to maintain the validity of the linear approximation. However, entropy-difference calculation does not rely on linear approximation; linear approximation in section 2.2 is adopted only to simplify our analysis. Entropy-difference is derived from the statistics of canopy reflectance data, either measured or simulated from the BRDF model. Thus, cases of nonlinear BRDF models and poor *a priori* knowledge can be analysed as well.

In this paper, we considered the homogeneous canopies that are described by the SAIL model and focused only on top-of-canopy reflectance data. In fact, the entropy-difference analysis can be adapted to any type of land cover provided there is a canopy reflectance model to link the surface parameters and the remote sensing measurement. Atmospheric effects can be considered in two possible ways: (1) to make atmospheric correction to remote sensing data and treat the correction error as noise; and (2) to use the coupled canopy-atmosphere canopy reflectance model. Future work should include a similar analysis for other canopies with other models, with and without atmospheric scattering.

The illumination of the entropy-difference method is based on simulated reflectance data from the canopy reflectance model. If the canopy model is suitable to describe the radiative process of the canopy, then it can be used to simulate the canopy reflectance data and select an optimal configuration. The factors related to the entropy-difference method, such as the *a priori* estimates and the canopy reflectance model, can affect the estimates of optimum view directions. Furthermore, different targets have different optimal angle/spectral combinations. However, the optimal angle selection method proposed here can be used for different canopy models and targets. Other canopy targets and models will be explored in the near future work.

5. Conclusion

With the growing number of satellite-borne multi-angular (e.g., MISR, ATSR) or wide-angle (e.g., MODIS, VEGETATION) sensors in operation, we face questions such as the following: Are more samples always better or is there a configuration with fewer number of samples but more information for model inversion? Entropy-difference is a powerful analysis tool for evaluating multi-angle reflectance data and for solving the multi-variable inversion problems. The method can be applied from the spectral point of view. We can see that the optimal configuration of two angles is actually better than numerous random configurations of three angles with respect to the LAI inversion. The entropy-difference method provides a quantitative criterion for judging canopy reflectance data. The reflectance data are fully exploited considering the information content within data.

Acknowledgements

This study was supported by Chinese Natural Science Foundation projects (40801125, 40871175, 40901280), Key Project of Chinese Natural Science Foundation (40730525), Knowledge Innovation Engineering Project of Chinese Academy of Sciences (KZCX2-YW-313), and open-funded project by State Key Laboratory of Remote Sensing Science.

References

Analytical Spectral Devices (ASD) 2000 FieldSpec pro user's guide.

Bicheron P and Leroy M 1999 A method of biophysical parameter retrieval at global scale by inversion of a vegetation reflectance model; *Remote Sens. Environ.* **67** 251–266.

Campbell G S 1985 Extinction coefficients for radiation in plant canopies calculated using an ellipsoidal inclination angle distribution; *Agri. Forest Meteorol.* **36** 317–321.

Canisius F, Fernandes R and Chen J 2010 Comparison and evaluation of Medium Resolution Imaging Spectrometer leaf area index products across a range of land use; *Remote Sens. Environ.* **114** 950–960.

Deng F, Chen J M, Plummer S, Chen M and Pisek J 2006 Algorithm for global leaf area index retrieval using satellite imagery; *IEEE Trans. Geosci. Remote Sens.* **44(8)** 2219–2229.

Gao F, Morisette J T, Wolfe R E, Ederer G, Pedelty J, Masuoka E, Myneni R, Tan B and Nightingale J 2008 An algorithm to produce temporally and spatially continuous MODIS-LAI time series; *IEEE Geosci. Remote Sens. Lett.* **5(1)** 60–64.

Gao W and Lesht B M 1997 Model inversion of satellite-measured reflectances for obtaining surface biophysical and bidirectional reflectance characteristics of grasslands; *Remote Sens. Environ.* **59** 461–471.

Goel N S and Strebel D E 1983 Inversion of vegetation canopy reflectance models for estimating agronomic variables: I. Problem definition and initial results using the Suit's model; *Remote Sens. Environ.* **13** 487–507.

Goel N S and Deering D 1989 Evaluation of a canopy reflectance model for LAI estimation through its inversion; *IEEE Trans. Geosci. Remote Sens.* **23** 674–684.

Jin Y F, Gao F, Schaaf C B, Li X, Strahler A H, Bruegge C J and Martonchik J V 2002 Improving MODIS surface BRDF/Albedo retrieval with MISR multi-angle observations; *IEEE Trans. Geosci. Remote Sens.* **40(7)** 1593–1604.

Li X, Gao F, Wang J and Strahler A 2001 *A priori* knowledge accumulation and its application to linear BRDF model inversion; *J. Geophys. Res.* **106(D11)** 11,925–11,935.

Lozano R, Baret F, Atauri I, Bertrand N, Auxiliadora Casterad M 2009 Optimal geometric configuration and algorithms for LAI indirect estimates under row canopies: The case of vineyards; *Agri. Forest Meteorol.* **149** 1307–1316.

Major D, Schaalje G, Wiegand C and Blad B 1992 Accuracy and sensitivity analysis of SAIL model-predicted reflectance of maize; *Remote Sens. Environ.* **41** 61–70.

Privette J L, Myneni R B, Emery W J and Hall F G 1996 Optimal sampling conditions for estimating grassland parameters via reflectance model inversions; *IEEE Trans. Geosci. Remote Sens.* **34(1)** 272–284.

Verhoef W 1984 Light scattering by leaf layers with application to canopy reflectance modeling: The SAIL model; *Remote Sens. Environ.* **16** 125–141.

Weiss M, Baret F, Myneni R B, Pragnère A and Knyazikhin Y 2000 Investigation of a model inversion technique to estimate canopy biophysical variables from spectral and directional reflectance data; *Agron.* **20** 3–22.

Woodbury Allan D and Ulrych T J 1993 Minimum relative entropy: Forward probabilistic modelling; *Water Resour. Res.* **29(8)** 2847–2860.

Yang P, Shibasaki R, Wu W, Zhou Q, Chen Z, Zha Y, Shi Y and Tang H 2007 Evaluation of MODIS Land Cover and LAI products in cropland of North China Plain using *in situ* measurements and Landsat TM images; *IEEE Trans. Geosci. Remote Sens.* **45(10)** 3087–3097.

Yao Y, Liu Q, Liu Q and Li X 2008 LAI retrievals and uncertainty evaluations for typical row-planted crops at different growth stages; *Remote Sens. Environ.* **112(1)** 94–106.

MS received 24 August 2011; revised 15 November 2011; accepted 29 December 2011